Korean J. Chem. Eng., 34(12), 3208-3213 (2017)
DOI: 10.1007/s11814-017-0223-x

pISSN: 0256-1115
eISSN: 1975-7220

Feasibility study on the differentiation between engineered and natural nanoparticles based on the elemental ratios

Woocheol Kim*, Changju Yeom*, Hyejin Lee*, Hwakyung Sung*,, Eunhye Jo**, Ig-chun Eom**, and Younghun Kim*,†**

*Department of Chemical Engineering, Kwangwoon University, 20 Kwangwoon-ro, Nowon-gu, Seoul 01897, Korea
**Department of Health Research, National Institute of Environmental Research, 42 Hwangkyung-ro, Seo-gu, Incheon 22689, Korea
(*Received 8 June 2017 • accepted 9 August 2017*)

Abstract−To understand the fate and exposure of engineered nanoparticles (ENPs) to environmental media, it is important to identify ENPs in the natural occurring nanoparticles (NNPs). Although nanomaterials have unique physical properties such as uniform particle size, hierarchical nanostructure, well-defined crystalline structure, and high surface area, compared to bulk materials, these properties are not suitable references to differentiate between ENPs and NNPs. Therefore, the identification and quantification of ENPs pose a big challenge to analysis. Herein, we did a feasibility study to distinguish between ENPs and NNPs based on the elemental ratio of target elements (Ti and Zn) to background elements (Fe and Al). Morphologies, particle size, and elemental analysis for 12 NNPs, 4 ENPs, and 3 NPs contained in consumer products were conducted. NPs were extracted from raw materials via density gradient ultracentrifugation and alkaline digestion. In a logarithm plot for the elemental ratio of {Ti+Zn} to {Ti/Zn}/{Fe+Al} and ternary plot of {Ti+Zn}, Fe, and Al ions for all samples, ENPs have a distinct contrast with NNPs. Therefore, it is expected that the suggested analysis for elemental ratio could be a preliminary screening tool to differentiate between ENPs and NNPs.

Keywords: Engineered Nanoparticles, Natural Nanoparticles, Nano-consumer Products, Density Gradient Ultracentrifugation, Alkaline Digestion

INTRODUCTION

The increasing manufacture and implementation of engineered nanoparticles (ENPs) will continue to lead to the release of these materials into the environment [1]. Although ENPs will certainly enter the environment through unintentional releases, the possible development and application of nanomaterials-based agrochemicals could lead to widespread intentional environmental dispersion [2]. Namely, this increasing use of ENPs in consumer products has raised concerns over its potential toxicity posed to both environmental and human systems [3]. Fortunately, extensive studies on in-vivo and in-vitro cytotoxicity of ENPs provide useful information about the nanotoxicity issues and human health risks, and the toxic effects were found to be primarily related to size, shape, surface properties and chemical compositions [4-6].

In addition, reliably assessing the environmental exposure risk of ENPs will depend highly on the ability to quantify and characterize these materials in environmental samples. Although numerous studies have been conducted on the fate and behavior of ENPs released into the environment, the knowledge base on the fate and toxicity to humans and ecosystems of naturally occurring nanoparticles is rather sparse [7]. The underlying mechanism and mode of interaction ENPs with bio-organisms to induce toxicity might be different from the interaction of cell surfaces with NNPs, which are often covered with natural organic matter. Therefore, a way has to be found to differentiate between NNPs and ENPs. However, due to a huge excess of NNPs in environment, the identification and quantification of ENPs pose a big challenge to analysis [8].

Distinguishing between engineered and naturally occurring nanoparticles requires improvement in the selectivity of nano-metrology, rather improvements in method sensitivity. Gulson and Wong reviewed the possibilities of isotopic labeling and tracking of ENPs (TiO_2, CdS, and ZnO) and partially proved the possible use of stable isotopes to monitor dermal absorption of zinc and titanium oxides in sunscreen preparations and other personal care products [9]. However, isotope tracing method was not proved to differentiate between ENPs and NNPs in environmental media. Since NNPs generally display a broader range of sizes, this difference in particle polydispersity between ENPs and NNPs may be useful for distinguishing between engineered and naturally occurring particles. However, transformation processes (dissolution, aggregation, and complexation) in environmental media will tend to alter the size distribution of ENPs [10], likely eliminating narrow size distributions as possible distinguishing property.

Nanoscale minerals may be composed of inorganic materials such as aluminosilicates (e.g., clay mineral) and metal oxides (e.g., iron and manganese oxyhydroxides) [11]. Thus, no NNPs has complete purity for composition elements, namely, their elemental ratio

†To whom correspondence should be addressed.
E-mail: korea1@kw.ac.kr

of component species was different with that of pure ENPs. Therefore, we investigated the possibility of differentiation between ENPs and NNPs based on the elemental ratio analysis of component elements. Natural mineral samples were collected from ilmenite-mining area and NNPs were separated from minerals by density gradient ultracentrifugation rate (DGUR) separation [12]. Reagent-level and manufactured TiO_2 and ZnO were selected as reference ENPs. In addition, NPs contained in nano-consumer products (sunblock and paint) were separated from products by alkaline digestion [13] and used as verification materials. Based on the elemental analysis for all materials, the possibility of differentiation of ENPs from NNPs was evaluated.

EXPERIMENTAL

1. Sample Preparation for NNPs and ENPs

The most common NNPs are soil colloids, which are constituted of silicate clay minerals, iron- or aluminum oxides/-hydroxides or humic organic matter, including black carbon. Therefore, natural mineral samples were collected from ilmenite-mining area, which is located in the Hadong, South Korea. 12 samples were collected from Jikjeon (site #1) and Wolhoeng (site #2) in south end and north end of Hadong, respectively. Ilmenite collected from Hadong is known to have mixed phase between rutile and Fe-oxide [14]. Reagent-ENPs (TiO_2 and ZnO) purchased from Sigma-Aldrich were of analytical grade and used as-received without further purification. Two ENPs were manufactured in the laboratory directly by reported methods. In the typical sol-gel process for manufactured-TiO_2 [15], 3 mM titanium butoxide and 160 mM ethylene glycol were used as precursor and reducing agent of hydrolysis rate, respectively. The mixture of two solutions was stirred for 8 h, followed by addition of 0.3% acetone. After annealing at 550 °C for 2 h, the spherical TiO_2 was obtained. Manufactured-ZnO was prepared by microwave-assisted method [16]. The mixture solution of 97 mM zinc nitrate and 12.5 mM sodium hydroxide was transferred into a 100 mL Teflon vessel, followed by microwave-heating (100 °C for 1 h) in a microwave reactor (MARS6, CEM) at 1.8 kW and 2.5 GHz of magnetron frequency. The obtained particles were dried at 80 °C in a drying oven for 24 h. These reagent- and manufactured-ENPs were selected as reference materials for analysis of elemental ratio of {Ti+Al} to other components. In addition, two-types of consumer products containing NPs (TiO_2 and/or ZnO), sunblock (Innisfree Co. and Amore-Pacific Co., Korea) and white-color paint (KSM6020, Noroo-paint Co., Korea), were selected and NPs were extracted by alkaline digestion.

2. Separation of NNPs by DGUR

In DGUR separation, the sample has a greater density than that of the highest density portion of the gradient. Because the centrifugal force can help particles to move radially away from the axis of rotation and can separate these particles by size and shape, the density of the fluid might affect the separation efficiency [12]. First, natural minerals were washed with deionized water (DW) and filtered with 75 μm stainless steel mesh to remove bulk particles. In the typical procedure, density gradient solutions (10-70%) of glycerin were prepared with deionized water (DW). A step gradient was created directly in centrifuge tubes (50 mL Falcon tube) by adding layers with increasing density to the bottom of the tube. A filtered mineral was immediately layered on top of the four-layer density gradient prior to ultracentrifugation. The typical centrifugation condition was 10 min at 22,000 rpm (53,029 ×g, SUPRA22, Hanil). The sample recovered in top layer was dried at 80 °C in a drying oven for 24 h.

3. Extraction of NPs from Consumer Products by Alkaline Digestion

To extract NPs from consumer products, alkaline digestion was used. Alkaline treatment has proven to yield high recoveries in terms of both particle number and total mass, relative to sonication-assisted homogenization and enzyme digestion. Alkaline digestion with tetramethylammonium hydroxide (TMAH) was shown to have high extraction efficiency of metallic nanoparticles, metal oxide, and carbon nanotubes [13]. Sunblock and paint samples were dried in an oven at 110 °C, and 10 mg quantity of dried samples was added into 1 mL of 25 wt% TMAH, and mixture was sonicated for 2 h. The resulting solution was five-times diluted with DW and filtered with Advantac paper (5 μm pore). After centrifugation three times with DW, final material was re-dispersed in DW.

4. Characterizations

After HNO_3 treatment of samples, the concentration of total elements (Ti, Zn, Al, and Fe) was measured with induced coupled plasma mass spectrometer (ICP-MS, iCAP-Q, ThermoFisher Scientific). The particle size distribution was analyzed by dynamic light scattering spectroscopy (DLS, ELS-Z, Photal) and transmission electron microscopy (TEM, JP/JEM-2010, Jeol). Surface morphology of samples was analyzed with field emission scanning electron spectrometer (FE-SEM, JSM-6700F, Jeol).

RESULT AND DISCUSSION

1. Separation of NPs from Raw Materials and its Characterizations

TiO_2 and ZnO NPs are manufactured worldwide in large quantities for cosmetics, especially sunblock, in which TiO_2 and ZnO NPs help protect the skin from UV light. Several articles have reported on the toxic effects of these NPs in animals, such as DNA damage [17], and cytotoxicity [18,19]. The nanowaste contained with TiO_2 and ZnO NPs was generally treated by wastewater treatment plant to remove their potential cytotoxicity. Therefore, the residual TiO_2 and ZnO in effluent could be released unintentionally into environmental media. Therefore, the fate of these materials should be studied to reduce and understand its nanotoxicity, and the starting point for the study on the environmental exposure of NPs is just differentiation between ENPs and NNPs. Herein, TiO_2 and ZnO were selected as target materials.

DGUR separation used in this work was based on the fact that the particles of different sizes that move with different velocities in the medium provide a basis for particle separation into distinct bands. This method was successfully applied to achieve length separation of SWCNT [20] and size and shape separation of metallic nanoparticles [12]. The density gradient of glycerin for four layer used here was 1.026-1.183 g/cm^3 for 10-70% layer. As shown in Fig. 1(a), natural mineral was filtered with micro-mesh to remove the bulk particles with micron-size. The fraction samples separated

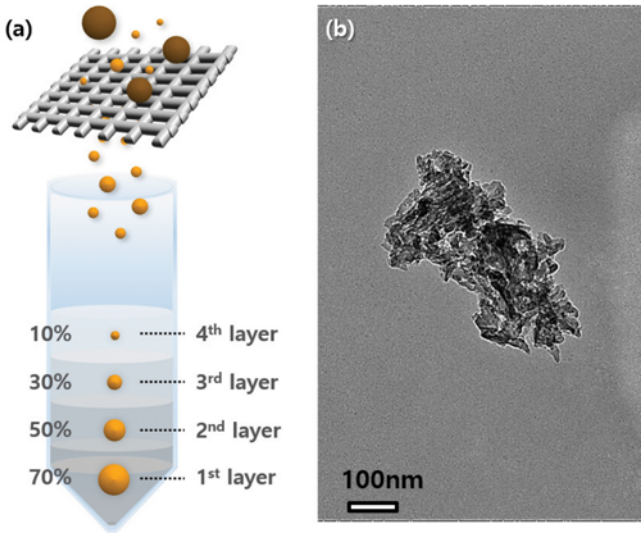

Fig. 1. (a) Extraction of natural nanoparticles by density gradient ultra-centrifugal separation and filtration, and (b) TEM image of natural nanoparticles (4th layer in glycerin-contained tube) separated from natural minerals.

from the fourth layer in tube have nanosized particles, and its size was confirmed with TEM and DLS analysis. As shown in Fig. 1(b), primary particles with ~100 nm were aggregated with neighboring particles and formed secondary large particle. Hydrodynamic diameter of secondary particle for 10, 30, 50, and 70% glycerin-layer was measured as 1,410, 1,211, 875, and 642 nm, respectively. Therefore, fraction recovered from the fourth layer was only used as NNPs samples.

Manufactured ENPs used here were prepared by well-known sol-gel and hydrothermal method. As reported in our previous work [16], homogeneous heating in microwave induced uniform nuclei growth without other impurity. Thus, low temperature and short heating time via microwave-assisted method was used to synthesize ZnO ENPs. As shown in Fig. 2(a), ZnO ENPs showed two-dimensional plate-like morphology with ~70 nm in thickness. This morphology of ZnO was found at another report [21]. Single plate of ZnO was aggregated and formed three-dimensional flower-like microstructure, as shown in inset figure in Fig. 2(a). This hierarchical ZnO has open porous structures for more efficient transportation for the reactant molecules into the active sites and to enhance the efficiency of photocatalyst [22]. In the case of TiO_2-ENPs, ethylene glycol was adjusted the hydrolysis rate of titanium precursor to fabricate titanium-glycolate intermediate precursor. On adding of intermediate in acetone, the glycolated precursor undergoes a slow hydrolysis and spherical titania particles are formed through homogeneous nucleation and growth process [23]. As shown in Fig. 2(b), the resulting TiO_2 NPs showed spherical particles with ~20 nm size. Reagent ENPs purchased from commercial band showed spherical and uniform nanostructure (Fig. 2(c) and 2(d)). Reagent TiO_2 and ZnO has ~29 and ~36 nm, respectively. Since these ENPs were used as received, their purity should be checked by ICP-MS analysis.

NPs contained in nano-consumer products (sunblock and paint) were recovered via extraction method using TMAH-digestion. In our previous work [13], while NaOH and KOH often cause particle aggregation, TMAH has high extraction yield without dissolution of NPs. Since TMAH is a very strong base and high pH

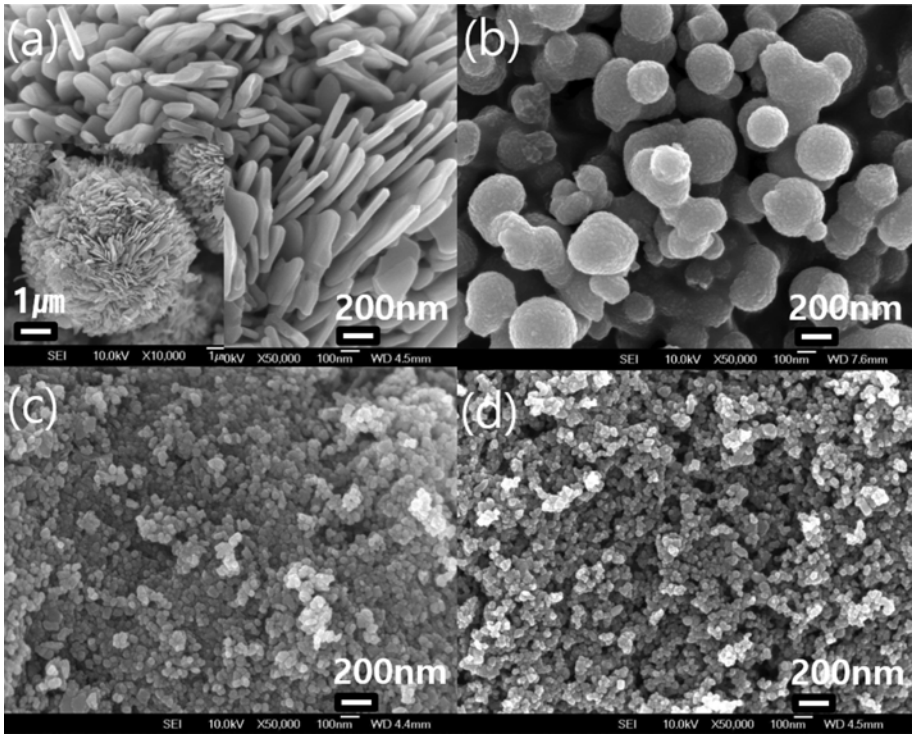

Fig. 2. SEM images of manufactured (a) ZnO and (b) TiO_2 nanoparticles, and reagent (c) ZnO and (d) TiO_2 nanoparticles.

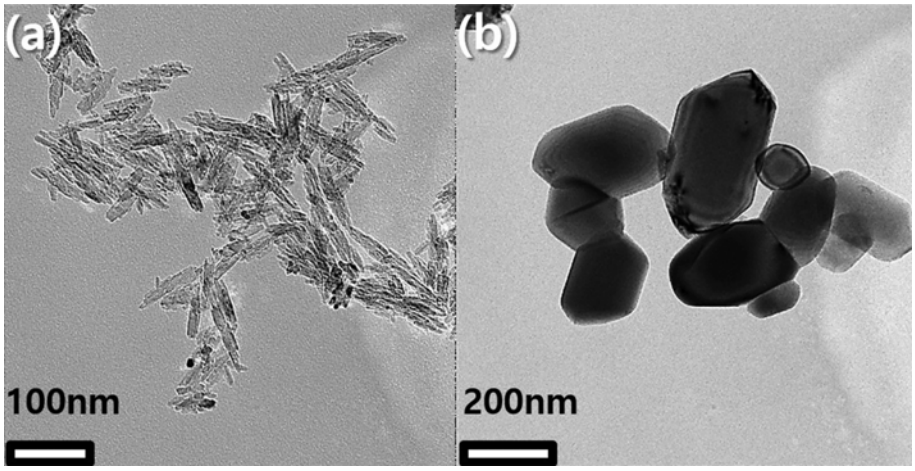

Fig. 3. TEM images of manufactured nanoparticles contained in (a) commercial sunblock and (b) white-color paint.

Table 1. Particle size of natural, manufactured and reagent samples

Compositions	Grade	Particle size (nm)	Measuring tools
TiO_2, ZnO	Natural NPs	642.3±44.3	TEM/DLS
TiO_2	Manufactured NPs	20.5±5.0	TEM/SEM
TiO_2	Reagent NPs	29.3±7.9	TEM/SEM
ZnO	Manufactured NPs	70.0±8.9 (thickness)	TEM/SEM
ZnO	Reagent NPs	36.1±10.3	TEM/SEM
TiO_2, ZnO	NPs in sunblock	68.5±18.0 (long)	TEM
		13.7±4.0 (short)	TEM
TiO_2	NPs in paint	228.8±73.1	TEM

conditions may induce the aggregation of neighboring NPs, pH of TMAH-treated solution should be adjusted neutral in order to obtain particulates that are not aggregated. After alkaline digestion, the resulting samples are recovered and analyzed for particle size and morphology by TEM. As shown in Fig. 3(a), NPs extracted from sunblock showed rod-like nanostructure with ~ 70 nm in length and ~14 nm in thickness. While, NPs extracted from paint have plate-like nanostructure with ~230 nm.

Particle size of natural, manufactured, reagent and extracted NPs is summarized in Table 1. All nanoparticles showed aggregated form in SEM images, but the primary particle ranged in nanometer scale from 10 to 100 nm. Particle size and polydispersity of samples was not correlated with whether NPs were engineered or naturally occurring. Note that these physical properties, such as size, polydispersity, and size distribution, were not suitable properties to differentiate between ENPs and NNPs. Manufactured ZnO has unique morphology, compared to other samples. It is obvious that plate-like or flower-like microstructure is artificially manufactured. However, many ENPs have a spherical shape and similar morphology with NNPs. Therefore, identification of ENPs from NNPs based on the morphological difference is also not acceptable.

2. Differentiation of ENPs and NNPs Using Elemental Ratio

Elemental compositions in the natural and manufactured samples vary widely depending on the preparation method, sampling spot, and synthetic conditions. Generally, manufactured ENPs have high purity of main components. Since NNPs have various mineral components, such as Al, Fe, Ti, and Zn, in natural conditions, the composition ratio was also different with pure ENPs. Therefore, elemental analysis for all samples was carried out using ICP-MS. As shown in Fig. 4(a), NNPs recovered from the fourth layer in Fig. 1(a) have four different elements (Ti, Zn, Fe, and Al). Silicon (26.8%), oxygen (47.4%), aluminum (8.4%) and iron (7.1%) are the most abundant element sin the earth's crust [11]. In this work, because silicon ion was not an interesting element, element analysis for Si ion was not conducted. The ilmenite ($FeTiO_3$) collected from Hadong as natural mineral showed large portion of Ti (site #2) but less-detectable Zn ion in NNPs. In site #1, average concentration of Ti, Zn, Fe, and Al elements was 78.14±25.94, 6.55±2.12, 938.19±342.08, and 1,297.59±757.06 mg/kg, respectively. In site #2, Ti, Zn, Fe, and Al showed 797.37±103.01, 13.6±8.47, 3,644.21±3,052.18, and 2,637.19±1,220.78 mg/kg, respectively. Namely, the composition ratio of {Fe+Al} and Ti in site #1 and site #2 is 96.3 and 3.4%, and 88.6 and 11.2%, respectively. Since the composition of Zn ion in natural mineral is 0.2% (site #2) and 0.3% (site #1) as minor element, if the concentration of Zn ion in unknown NPs whether ENPs or NNPs has some significance value compared to other elements (Ti, Fe, and Al), those NPs may be referred to as ENPs.

Fig. 4(b) represents the concentration of Ti, Zn, Fe, and Al contained in reagent-/manufactured-ENPs and consumer products. Reagent- and manufactured-ENPs have a high purity for Ti and Zn ion in TiO_2 and ZnO. Whereas, NPs contained in consumer

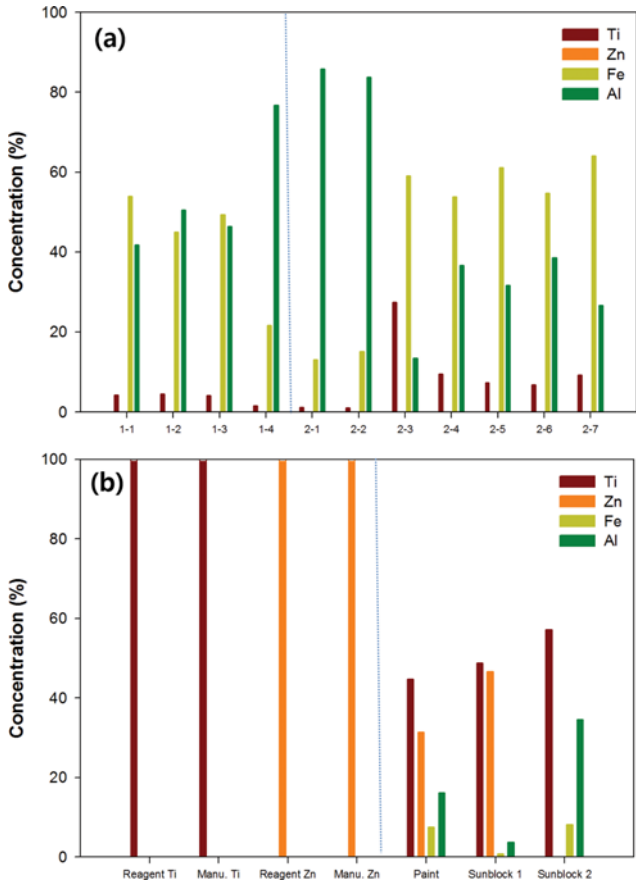

Fig. 4. Elemental compositions of Ti, Zn, Fe, and Al in the (a) natural and (b) manufactured samples. Natural nanoparticles in (a) were recovered from the 4th layer as shown in Fig. 1(a).

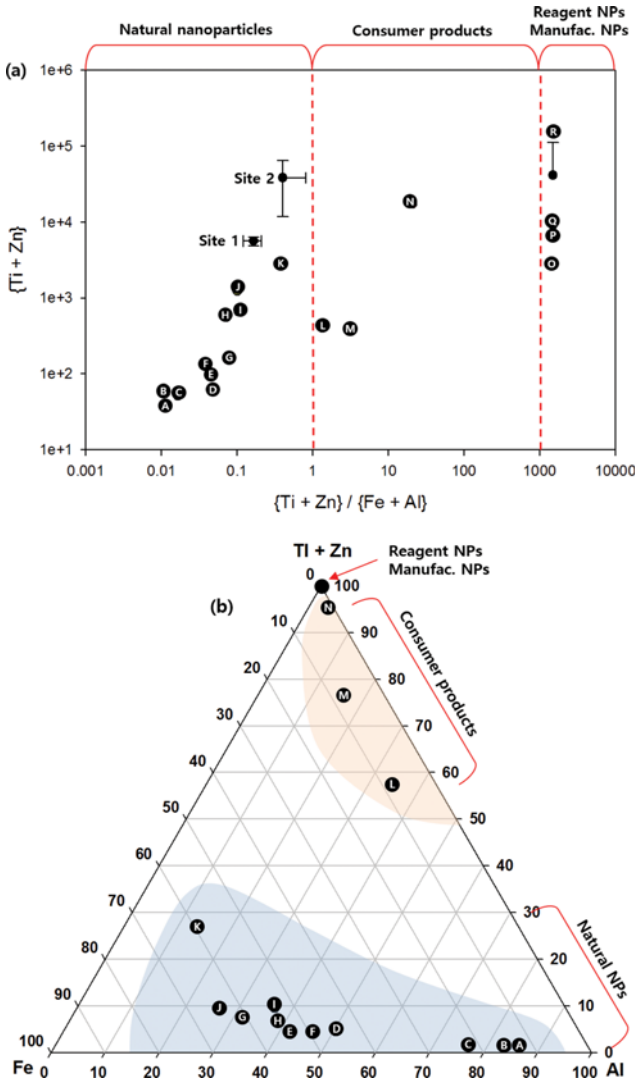

Fig. 5. (a) Logarithm plot for the elemental ratios of {Ti+Zn} to {Ti+Zn}/{Fe+Al} in all samples. (b) Triangular diagram for the element compositions of Ti, Zn, Fe, and Al species in all samples. A: 2-1, B: 2-2, C: 1-4, D: 1-2, E: 1-1, F: 1-3, G: 2-5, H: 2-6, I: 2-4, J: 2-7, K: 2-3, L: sunblock 1, M: paint, N: sunblock 2, O: manufactured ZnO, P: reagent TiO_2, Q: reagent ZnO, R: manufactured TiO_2, site 1: Wolhoeng-ri, site 2: Jikjeon-ri.

products showed various composition of Ti, Zn, Fe, and Al elements. The composition of Ti, Zn, Fe, and Al elements in paint is 44.8, 31.5, 7.6, and 16.2%, respectively. Sunblock 1 and 2 showed 48.8, 46.7, 0.9, and 3.7%, and 56.8, 0.7, 8.2, and 34.3%, for Ti, Zn, Fe, and Al elements, respectively. Based on the elemental analysis, paint and sunblock 1 contain a mixture of TiO_2 and ZnO ENPs, while sunblock 2 contains TiO_2 ENPs without ZnO. Trace materials for sunblock 1 and 2 were known as aluminum hydroxide, hydrated ferric oxide, alumina, and aluminum stearate, which was identified as cosmetic component manual.

For more specific distinction between ENPs and NNPs, the elemental ratio of {Ti+Zn} to {Ti/Zn}/{Fe+Al} for all samples is represented as a logarithm plot in Fig. 5(a). Analytical methodology for the elemental ratio was found in the study on the release of TiO_2 NPs from sunscreens into surface waters. Gondikas et al. [24] found that the Ti/Al ratio was significantly different between the summer and spring, and this difference was due to the heavily used TiO_2-contained sunscreens for recreational activities like bathing and water sports during the summer season. Elemental ratio of {Ti+Zn} was increased with decreasing of background elements {Fe+Al}, and thus {Ti+Zn} show linearized correlation with {Ti/Zn}/{Fe+Al} ratio. Site #1 and #2 points in Fig. 5(a) revealed the average elemental ratio of natural mineral without post-treatments (filtration and DGUR). While {Ti/Zn}/{Fe+Al} ratio of NNPs ranged in 0.01 to 1, its ratio of NPs extracted from consumer products was from 1 to 100. Pure ENPs such as reagent- and manufactured-TiO_2 and ZnO showed above value of 100 in {Ti/Zn}/{Fe+Al} ratio. Additionally, element compositions for Ti, Zn, Fe, and Al in NPs were represented as other form like a triangular diagram as shown in Fig. 5(b). Ternary plot for {Ti+Zn}, Fe, and Al ions was helpful to identify the composition ratio at a glance. Since NNPs with high composition of Fe and Al, NNPs sampled from Hadong were located in the bottom range of 0 to 30% {Ti+Zn}. NPs extracted from consumer products have high concentrations of Ti and Zn compared to Fe and Al, and thus points located in the top range of 50 to 95% {Ti+Zn}. Pure ENPs exhibit in the vertex of {Ti+Zn}.

Single-particle ICP-MS (SP-ICP-MS) and crystallinity analysis

using X-ray diffractometer (XRD) could be candidates as another differentiation methodology between ENPs and NNPs. As pointed out by Gondikas et al. [24], SP-ICP-MS currently cannot measure more than one isotope simultaneously and crystal structural differences between ENPs and NNPs are not particularly promising. Although isotopic analysis has been successfully used with other elements, such as mercury to trace their source to manufacturing processes [25], this method is also not likely to be useful in the case of TiO_2 due to the quantitative conversion of the source materials to ENPs [26]. Therefore, given these limitations, the elemental ratio of specific elements in samples to use locally established background elemental ratios seems to be the candidate solution for differentiation between ENPs and NNPs.

CONCLUSIONS

We investigated the possibility of differentiation between ENPs and NNPs based on the elemental ratio analysis of component elements. Natural mineral samples were collected from ilmenite-mining area, which is located in Hadong, Korea, and 12 NNPs were separated from minerals by DGUR separation. Reagent- and manufactured-TiO_2 and ZnO were selected as reference ENPs, and additionally, 3 NPs samples were extracted from nano-consumer products (sunblock and paint). Based on the analysis of particle size and polydispersity of samples, these physical properties were not suitable properties to differentiate between ENPs and NNPs. Elemental analysis for all samples was carried out using ICP-MS, and elemental ratio of {Ti+Zn} to {Ti/Zn}/{Fe+Al} for ENPs showed a distinct difference with that for NNPs. While {Ti/Zn}/{Fe+Al} ratio of NNPs ranged in 0.01 to 1, its ratio of NPs extracted from consumer products was from 1 to 100, and reagent-/manufactured-ENPs such as reagent- and manufactured-TiO_2 and ZnO showed above value of 100 in {Ti/Zn}/{Fe+Al} ratio. In addition, a ternary plot for {Ti+Zn}, Fe, and Al ions was helpful in identifying the composition ratio at a glance. Based on a feasibility test for distinguishing ENPs from NNPs, the elemental analysis of specific elements to background elemental ratios might be candidates for differentiation between ENPs and NNPs.

ACKNOWLEDGEMENTS

This study was supported by the Research Grant from the National Institute of Environmental Research, and the National Research Foundation of Korea (NRF-2017R1A2B4001829).

REFERENCES

1. M. D. Montano, G. V. Lowry, F. von der Kammer, J. Blue and J. F. Ranville, *Environ. Chem.*, **11**, 351 (2014).
2. B. Nowack and T. D. Bucheli, *Environ. Pollut.*, **150**, 5 (2007).
3. J. S. Hong, S. Kim, S. H. Lee, E. Jo, B. Lee, J. Yoon, I. C. Eom, H. M. Kim, P. Kim, K. Choi, M. Y. Lee, Y. R. Seo, Y. Kim, Y. Lee, J. Choi and K. Park, *Nanotoxicology*, **8**, 349 (2014).
4. E. Bae, B. C. Lee, Y. Kim, K. Choi and J. Yi, *Korean J. Chem. Eng.*, **30**, 364 (2013).
5. E. S. Bernhardt, B. P. Colman, M. F. Hochella Jr., B. J. Cardinale, R. M. Nisbet, C. J. Richardson and L. Yin, *J. Environ. Qual.*, **39**, 1 (2010).
6. E. J. Park, H. Kim, Y. Kim, J. Yi, K. Choi and K. Park, *Toxicol.*, **275**, 65 (2010).
7. V. K. Sharma, J. Filip, R. Zboril and R. S. Varma, *Chem. Soc. Rev.*, **44**, 8410 (2015).
8. H. Znaker and A. Schierz, *Annu. Rev. Anal. Chem.*, **5**, 107 (2012).
9. B. Gulson and H. Wong, *Environ. Health Perspect.*, **114**, 1486 (2006).
10. G. V. Lowry, K. B. Gregory, S. C. Apte and J. R. Lead, *Environ. Sci. Technol.*, **46**, 6893 (2012).
11. M. Abd El-Rahman, M. F. El-Khadragy, H. Adb-El Hay and D. N. Gab-Allah, *J. Hazard. Mater.*, **186**, 1527 (2011).
12. J. H. Sim, H. N. Umh, H. H. Shin, H. K. Sung, S. Y. Oh, B. C. Lee, R. Selvaraj and Y. Kim, *J. Ind. Eng. Chem.*, **20**, 3157 (2014).
13. S. Park and Y. Kim, *J. Ind. Eng. Chem.*, **41**, 62 (2016).
14. J. Y. Kwak and J. B. Choi, *J. Miner. Soc. Korea*, **27**, 197 (2014).
15. D. Chen and R. A. Caruso, *Adv. Funct. Mater.*, **23**, 1356 (2013).
16. S. Park, R. Selvaraj, M. A. Meetani and Y. Kim, *J. Ind. Eng. Chem.*, **45**, 206 (2017).
17. B. Trouiller, R. Reliene, A. Westbrook, P. Solaimani and R. H. Schiestl, *Cancer Res.*, **69**, 8784 (2009).
18. J. Lee, J. Kim, Y. Shin, J. Ryu, I. C. Eom, J. S. Lee, Y. Kim, P. Kim, K. H. Choi and B. C. Lee, *Ecotoxicol. Environ. Safety*, **104**, 9 (2014).
19. U. Song, M. Shin, G. Lee, J. Roh, Y. Kim and E. J. Lee, *Biol. Trace Elem. Res.*, **155**, 93 (2013).
20. M. S. Arnoid, A. A. Green, J. F. Hulvat, S. I. Stupp and M. C. Hersam, *Nat. Nanotechnol.*, **1**, 60 (2006).
21. Y. Lu, L. Wang, D. Wang, T. Xie, L. Chen and Y. Lin, *Mater. Chem. Phys.*, **129**, 281 (2011).
22. S. Park, J. Park, S. Rengaraj and Y. Kim, *J. Ind. Eng. Chem.*, **31**, 269 (2015).
23. M. Pal, J. G. Serrano, P. Santiago and U. Pal, *J. Phys. Chem. C*, **111**, 96 (2007).
24. A. P. Gondikas, F. von der Kammer, R. B. Reed, S. Wagner, J. F. Ranville and T. Hofmann, *Environ. Sci. Technol.*, **48**, 5415 (2014).
25. G. Bartov, A. Deonarine, T. M. Johnson, L. Ruhl, A. Vengosh and H. Hsu-Kim, *Environ. Sci. Technol.*, **47**, 2092 (2013).
26. S. J. Klaines, A. A. Koelmans, N. Horne, S. Carley, R. D. Handy, L. Kapustka, B. Nowack and F. von der Kammer, *Environ. Toxicol. Chem.*, **31**, 3 (2012).